



Impact of SRTM and Corine Land Cover data on meteorological parameters using WRF



A. De Meij*, J.F. Vinuesa

Noveltis, Sustainable Development, 153, Rue du Lac, F-31670 Labege, France

ARTICLE INFO

Article history:

Received 20 September 2013

Received in revised form 6 March 2014

Accepted 9 March 2014

Available online 16 March 2014

Keywords:

WRF

Corine Land Cover

SRTM

USGS Land Cover

ABSTRACT

The objective of this study is to evaluate the impact of the high resolution SRTM topography and Corine Land Cover data on simulated meteorological variables (wind speed at ten metres height, temperature at 2 m height and precipitation) in WRF. We compare the results with the WRF simulation using the standard 30-arc second USGS Land Cover and topography, and with observations of the ARPA network. We focus on the Lombardy region (north Italy) for the periods January–February and July–August 2008.

Our analysis shows that simulated average wind speeds are in general lower by the WRF simulation with the SRTM and Corine Land Cover than the WRF simulation with the 30-arc second USGS and agrees better with the observations. The reason for this is that the Corine Land Cover shows a larger fraction of the 'urban and built-up' category than the USGS data set, which leads to more friction and higher roughness in the domain and lowers the wind speeds at ground level. For the winter period, the WRF simulation with the SRTM and Corine Land Cover calculates on average higher temperatures over the model domain (between ~0.2 and ~1.0 °C and up to ~1.2 °C for Milan) than the simulation using USGS data. For the summer period the differences in average temperatures are larger up to 2.7 °C, while for Milan the differences are around 0.7 °C. The differences are related to the higher fraction of urban and built-up area in the Corine Land Cover, which affects the sensible and latent heat fluxes in the model domain and holds the heat between the buildings. R² values are on average a factor of 1.03 and 1.14 higher for the winter and summer periods, respectively. Comparing the hit rate statistics of the precipitation events reveals that probability of detection of the precipitation event and the Hansen–Kuipers score is on average 1% higher by the simulation with SRTM and Corine Land Cover than the WRF simulation with the standard USGS data set.

© 2014 Elsevier B.V. All rights reserved.

1. Introduction

A common problem in air quality modelling is the underestimation of particulate matter (PM) simulated values by air chemistry transport models (ACTMs). Several model studies (Tsyro, 2003; Van Loon et al., 2004; De Meij et al., 2007, 2008, 2009a; Vautard et al., 2007, 2009; Stern et al., 2008), and coordinated modelling activities such as AEROCOM [<http://aerocom.met.no/aerocomhome.html>], Eurodelta [<http://aqm.jrc.ec.europa.eu/eurodelta/>]] and Citydelta [<http://aqm.jrc.ec.europa.eu/citydelta/>], showed that models in general underestimate observed PM concentrations over Europe. In Textor et al. (2006) and De Meij (2009b) several reasons are given for the underestimation of particulate matter (PM) concentrations, such as uncertainties in the estimation of gases and primary aerosols in the emission inventories, aerosol dynamics (physical transformations, dry and wet removal, transport) and meteorological factors (temperature, humidity, wind speed and direction, precipitation, cloud chemistry, vertical mixing).

Meteorological input data is simulated by a meteorological model and serves as input for the ACTM. The ACTM

* Corresponding author.

E-mail address: alexander.demeij@noveltis.fr (A. De Meij).

requires a set of meteorological parameters (e.g. temperature, wind velocity, absolute and relative humidity, pressure, air density, heat fluxes) to calculate transport, diffusion, chemistry and formation and removal mechanisms of gas and aerosol pollutants. Aerosol formation processes are known to be nonlinearly dependent on meteorological parameters such as temperature, humidity and vertical mixing (Haywood and Ramaswamy, 1998; Penner et al., 1998) and the concentrations of precursor gases (West et al., 1998). Several studies have shown the importance of topography and meteorology on simulated gas and aerosol concentrations. Minguzzi et al. (2005) studied the impact of different meteorological inputs on model sensitivity calculations. In this study the wind fields were varied, which lead to significant differences in calculate ozone and PM10 concentrations in urban areas. Carvalho et al. (2006) performed a pollutant dispersion study over a complex terrain with the meteorological driver MM5 and concluded that topography represents the most important factor of transport of atmospheric pollutants e.g. ozone, to higher altitude. The City Delta exercise (<http://aqm.jrc.ec.europa.eu/citydelta/>, Cuvelier et al., 2006; Thunis et al., 2007; Vautard et al., 2006) showed that simulated PM concentrations are underestimated by the ACTMs for Milan (Italy), especially for winter time episodes. The Po Valley is characterized by very low wind speeds and frequent weak circulation conditions. These stagnant meteorological conditions are difficult to simulate by prognostic and diagnostic models over complex areas (Dosio et al., 2002; Minguzzi et al., 2005; Carvalho et al., 2006; Stern et al., 2008; De Meij et al., 2009a; Ritter et al., 2013), which lead to the underestimation of simulated PM concentrations. The accuracy of land-use classifications in meteorological modelling affects some meteorological parameters such as wind fields and temperature near the surface (Lee et al., 2010). Urban built-up areas are more likely to trap incoming radiation and wind profiles than open rural areas, which may impact the temperatures, buoyancy and wind directions and wind speeds. A good estimate of meteorological variables in the meteorological data sets is therefore crucial for calculating gas and aerosol impacts on air quality and climate change, and evaluating coherent reduction strategies.

A recent study by Kim et al. (2013) studied the impact of different planetary boundary layer (PBL) schemes and the 250×250 m resolution Corine Land Cover on meteorological parameters (e.g. wind speed, planetary boundary layer development, relative humidity and temperature) in the Weather Research and Forecasting model (WRF, <http://wrf-model.org/index.php>) over the Paris area. They found that the simulations with the Corine Land Cover improved to some extent the simulated temperature profiles, but larger improvements were found for the simulated wind speeds and relative humidity values and especially the nocturnal PBL heights. They also found that the impact of the urban canopy model together with the Corine Land Cover showed a larger impact on the simulated meteorological variables in WRF than changing the PBL schemes. Therefore increasing the land-use spatial resolution could partly solve the issue of underestimated PM concentrations in ACTMs.

In this study, we investigate the impact of the high resolution Shuttle Radar Topography Mission (SRTM) 90 m topography data (Farr et al., 2007; Jarvis et al., 2008) together with the Corine Land Cover 2006 (Heymann et al., 1994;

Büttner et al., 1998, 2002.) at 100×100 m resolution on the simulated wind, temperature and precipitation profiles by WRF. Corine stands for COordination of INformation on the Environment. In order to investigate the impact of the SRTM together with the Corine Land Cover we compare the simulated meteorological parameters with the results of the WRF simulation using the standard 30-arc second USGS Land Cover and topography (Anderson et al., 1976) and with observations of the ARPA network. We focus on the southern region of the Alps, more specifically the Lombardy region, because (i) this area showed to be problematic in previous aerosol modelling studies, (ii) the Po valley is one of the most polluted, industrialized and densely populated areas in Europe and (iii) this area shows a large diversity in land cover. It contains several big lakes and mountains and the region is highly populated (ISTAT, 2012). In Fig. 1 a subset of the Lombardy region is shown with Milan city clearly visible in the centre of the figure (red), together with Lake Maggiore and Lake Como. More details about WRF, SRTM topography and Corine Land Cover are given in Section 2.

2. Methodology

The WRF model is used over a part of the Po Valley area (north Italy) to study the impact of high SRTM topography and Corine Land Cover on the simulated meteorological variables wind speed, precipitation and temperature at two metres (2 m). More details regarding the meteorological model are given in Section 2.1.

WRF operates on the 5×5 km and 1×1 km resolution domains (two-way nested i.e. feedback from nest to its parent domain). Fig. 1B presents the geographical position of the model grid domains. Four simulations were performed with no nudging to the observations of the meteorological stations (Table 1a). The first simulation uses the SRTM and Corine Land Cover data for the period January–February 2008. The second simulation uses the standard USGS 30-arc second land-use data ($\sim 1 \times 1$ km) and topography data for the same period. The third and fourth simulations are similar as described earlier, but for the period July–August 2008. Both periods (January–February and July–August) are average wet periods, with October and November as the wettest periods. On the other hand January–February and July–August are considered as the coldest and warmest periods, respectively. The simulations with SRTM and Corine Land Cover are further denoted as WRF_CLCW and WRF_CLCS (winter and summer respectively), the simulations with 30-arc seconds are further denoted as WRF_30sW and WRF_30sS (winter and summer, respectively). We compare the simulated values with meteorological observations given by the monitoring network of the Regional Agencies for Environment Protection in Lombardy (Agenzia Regionale per la Protezione dell' Ambiente, ARPA Lombardia, www.arpalombardia.it). Through this website the following parameters can be downloaded: precipitation, temperature, atmospheric pressure, wind speed and wind direction, relative humidity, global irradiation and net irradiation. The statistical analysis of the simulated meteorological values and the observations used in this work is based on hourly values. The numbers of observations for a meteorological parameter may differ from one station to the other, depending on the amount of observations available.

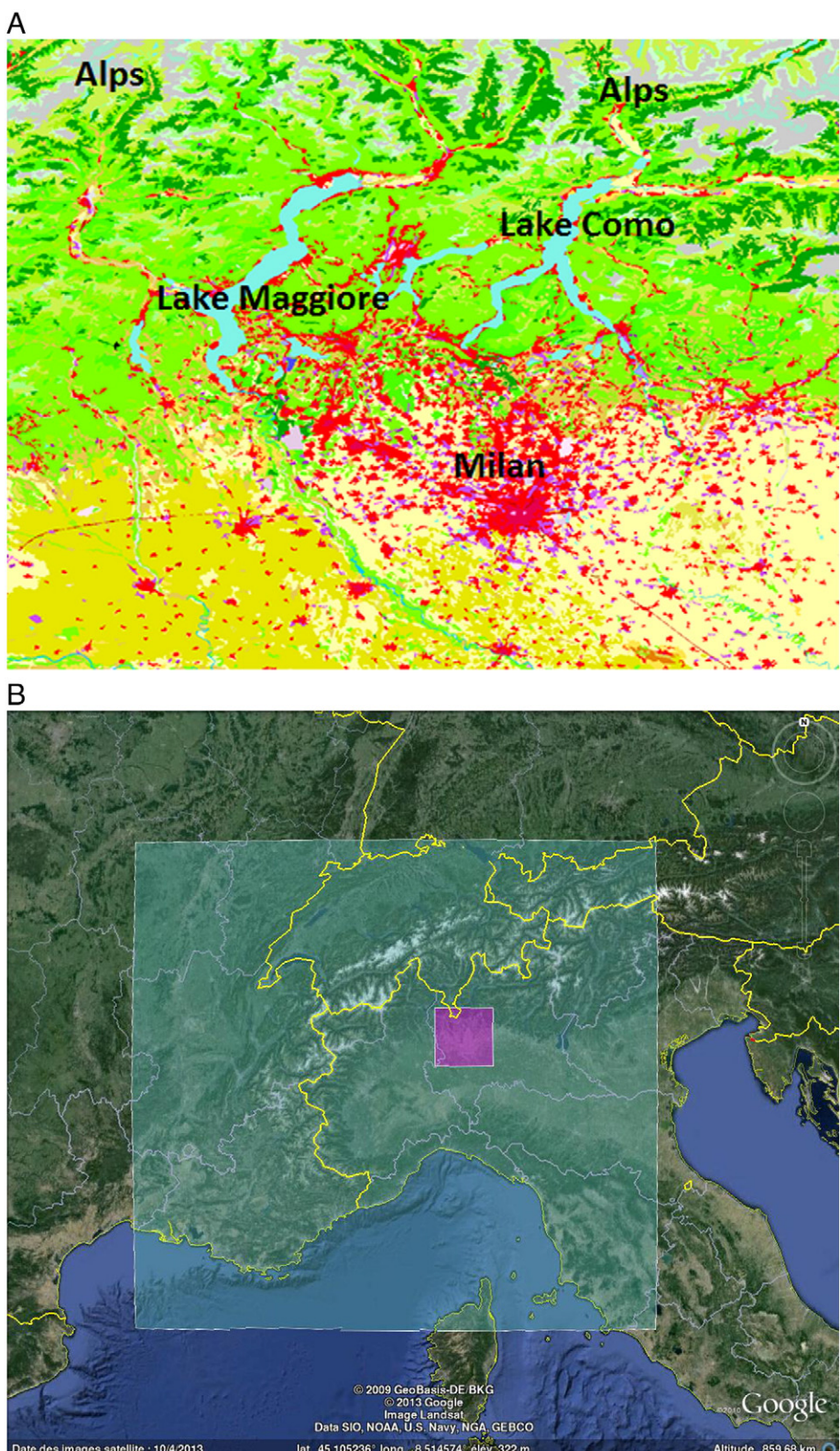


Fig. 1. A. A subset of the Corine Land Cover (100×100 m) over northern Italy and Alps. The red colour represents urban land-use (with the city of Milan centre right), dark green forest land, light green grasslands, violet industrial areas, light blue water bodies, grey open spaces/bare soils, olive green arable land and permanent crops. B. Map of the locations of the two WRF model domains. The larger domain has a horizontal spatial resolution of 5×5 km, and the smaller domain has a horizontal resolution of 1×1 km. Photo courtesy Google Earth™ mapping service.

Table 1a

Overview of the type of simulations performed in this study.

Type of simulation	Type of topography and land-use	Denoted in the study
January–February 2008	SRTM and Corine Land Cover	WRF_CLCW
January–February 2008	USGS	WRF_30sW
July–August 2008	SRTM and Corine Land Cover	WRF_CLCS
July–August 2008	USGS	WRF_30sS

For the simulations, a spin-up time of four days is applied in order to initialize the model. WRF uses meteorological initial conditions and lateral boundary conditions from 6 hour analyses from the National Centers for Environmental Protection (NCEP; Kalnay et al., 1996) Climate Forecast System Reanalysis (CFSR; Saha et al., 2010).

2.1. Description WRF

The WRF-ARW system is a non-hydrostatic model (with a hydrostatic option) using terrain-following vertical coordinate based on hydrostatic pressure. The terrestrial data sets for the WRF model are built using the NCEP geographical data. These consist in global data sets for soil categories, land-use, terrain height, annual mean deep soil temperature, monthly vegetation fraction, monthly albedo, maximum snow albedo and slopes.

The resolution used for implementing land-use in the proposed study is based on (i) the Corine 2006 Land Cover data set (100×100 m) and (ii) the 30-arc second United States Geological Survey (USGS) database. WRF uses land-use categories from USGS 24-category data, which are available for different horizontal resolutions (10', 5', 2', 30"; 'denotes arc seconds and 'denotes arc minutes). The horizontal resolution is set by the user in the pre-processing step in WPS. The highest horizontal resolution available in the USGS land-use is 30",

which corresponds to $\sim 1 \times 1$ km. The USGS land-use data was created in 1993, since then urban areas have changed significantly for some regions in Europe. The Corine Land Cover is a European Commission program, started in 1985 by the European Commission DG Environment, intended to provide consistent localized geographical information on the land cover of the Member States of the European Community. The Corine Land Cover is recognised by decision-makers as an essential reference data set for spatial and territorial analyses on different territorial levels (Büttner et al., 2002). To make the Corine Land Cover categories (44) compatible with WRF Pre-processing System (WPS) the Corine Land Cover is reclassified to the USGS category (24 land-use categories, Pineda et al., 2004). The Corine Land Cover data set is projected on the European Terrestrial Reference System 1989 (ETRS89) Lambert Azimuthal Equal Area (LAEA), which is not compatible with the WRF system. Therefore the Corine Land Cover is re-projected to the World Geodetic coordinate System 1984 (WGS84) Arnold et al. (2010). Table 1b shows the 24 land-use categories in the USGS database. The Corine Land Cover data set can be found on: <http://www.eea.europa.eu/data-and-maps/data/corine-land-cover-2006-raster-2>.

For the simulation with the Corine Land Cover, we also implemented the Shuttle Radar Topography Mission (SRTM) in WPS. This allows us to make a fair comparison between the simulation with the default USGS Land Cover and topography data, which are both on a resolution of 30". The SRTM flew aboard the Space Shuttle Endeavour, which obtained terrain elevation data during an eleven day mission in February of 2000 to generate the most complete high-resolution (~ 90 m) digital topographic database of Earth. High resolution SRTM data can be found on <http://srtm.csi.cgiar.org/SELECTION/inputCoord.asp>.

The vertical discretization of WRF involves 28 levels up to about 18 km. The same model set up is applied, i.e. microphysics and dynamics options are the same for the four model

Table 1b

USGS 24 land use categories, together with the amount of cells in the model domain for the USGS and Corine Land Cover.

USGS land use category	Land use description	# cells in the USGS Land Use	# cells in the Corine Land Cover
1	Urban and built-up land	200	3370
2	Dryland cropland and pasture	3465	3040
3	Irrigated cropland and pasture	537	565
4	Mixed dryland/irrigated cropland and pasture	0	0
5	Cropland/grassland mosaic	118	0
6	Cropland/woodland mosaic	527	1273
7	Grassland	3	117
8	Shrubland	3	0
9	Mixed shrubland/grassland	0	131
10	Savanna	0	0
11	Deciduous broadleaf forest	411	1504
12	Deciduous needleleaf forest	0	0
13	Evergreen broadleaf	0	0
14	Evergreen needleleaf	8	170
15	Mixed forest	131	911
16	Water bodies	243	286
17	Herbaceous wetland	0	40
18	Wooden wetland	0	0
19	Barren or sparsely vegetated	0	65
20	Herbaceous tundra	0	0
21	Wooded tundra	0	0
22	Mixed tundra	0	0
23	Bare ground tundra	0	0
24	Snow or ice	0	0

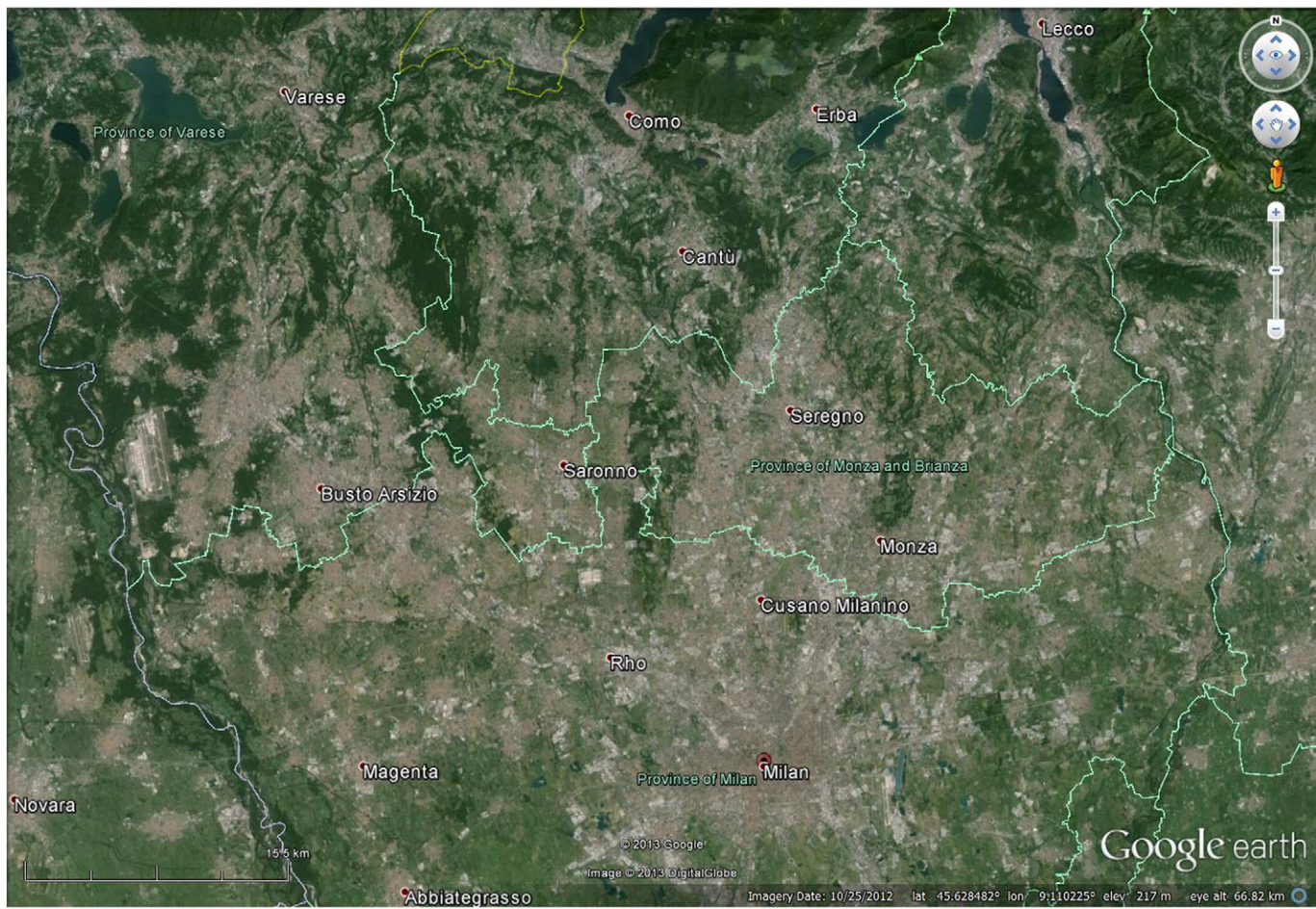


Fig. 2. Google Earth image of the model domain (North Italy, Milan region). The grey areas depict mainly the urban built-up areas. Photo courtesy Google Earth™ mapping service.

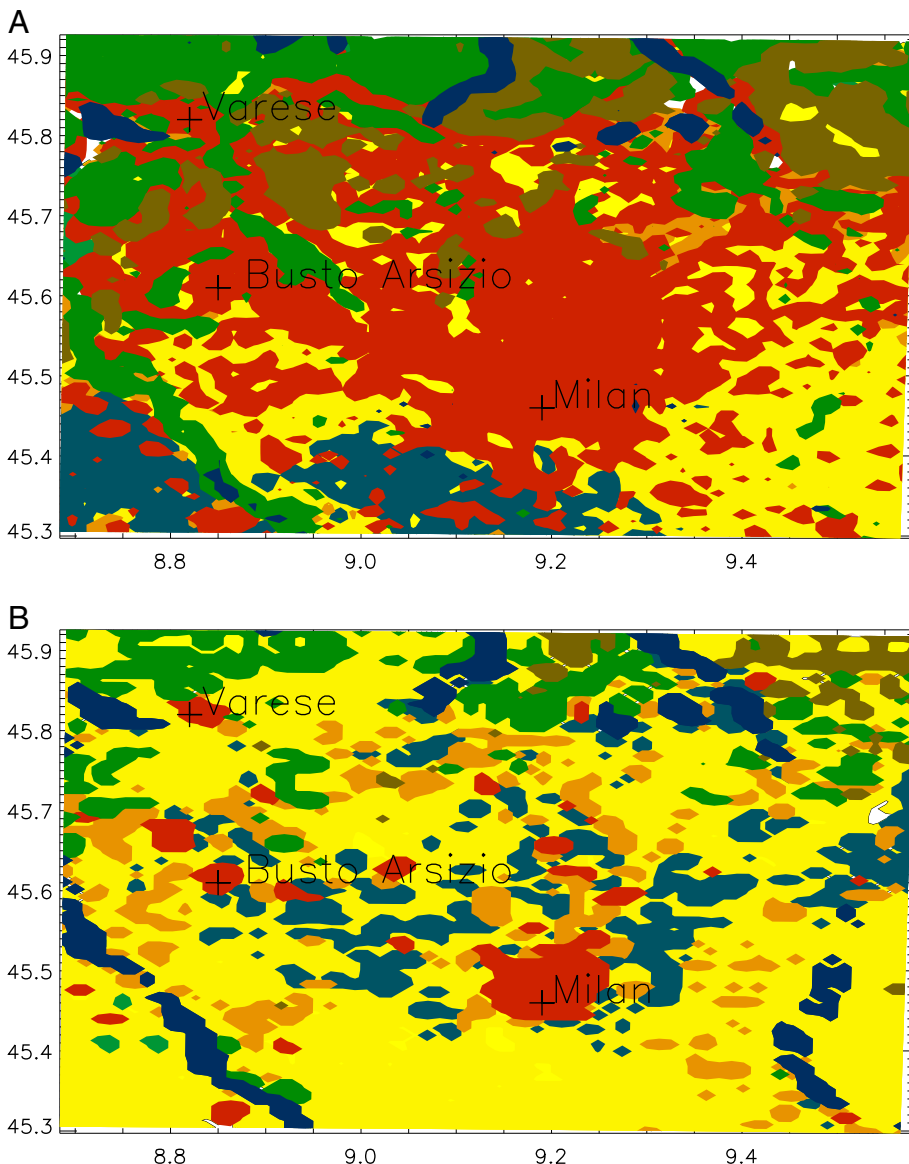


Fig. 3. Contours of the land-use category classes in Corine Land Cover (A) and USGS (B). Red colour represents the Urban and Built-Up Land land-use category, yellow dry cropland and pasture, grey/blue irrigated cropland and pasture, dark blue water bodies, light brown crops/wood, dark green mixed forest, green deciduous broadleaf forest and evergreen needle leaf forest and white represent the other remaining land-use categories.

simulations. The model is set up using single-moment six class microphysics scheme (WSM6) containing ice, snow and graupel processes, vapour, and rain (mixed-phase processes, appropriate for the analyzed range of spatial horizontal resolutions finer than 5 km, Hong and Lim, 2006). It uses the Noah land surface model scheme (Chen and Dudhia, 2001) with soil temperature and moisture in four layers, fractional snow cover and frozen soil physics and provides heat and moisture fluxes for the PBL. The PBL Yonsei University (YSU) scheme is used to set up the model (Hong et al., 2006). The long wave radiation is simulated by the RRTM scheme (Mlawer et al., 1997). The default diffusion scheme is selected. The short wave radiation is simulated by the New Goddard scheme

(Chou and Suarez, 1999, NASA Tech Memo). The cumulus scheme is not activated for the two resolutions. It is recommended to activate the cumulus scheme on coarser grids e.g. $>10 \times 10$ km, when it is not resolved by the model (http://www.dtcenter.org/wrf-nmm/users/docs/user_guide/V3/users_guide_nmm_chap5.pdf).

2.2. Differences in land-use between Corine Land Cover and USGS land cover

The land cover in the domain of the reclassified Corine Land Cover data set is mainly dominated by urban and built-up cover, while in the 30" USGS the Urban and Built-Up

category is only concentrated around the larger cities, such as Milan, Varese and Busto Arsizio. It is well known that the area around these cities is highly populated; a Google Earth screenshot in Fig. 2 illustrates the densely populated region. The higher fraction of urban area produces more resistance by the buildings (roughness), which reduces the wind speeds. This corroborates the study by Kim et al. (2013). They found a higher fraction of the urban and built-up category in the Corine Land Cover for the Paris area than in USGS.

To illustrate additional differences in the land cover categories between the Corine Land Cover and the 30" USGS databases we show in Fig. 3 the distribution of the dry cropland and pasture, irrigated cropland and pasture and water bodies. These are land-use categories two, three and 16 in the USGS data set. As for the differences in urban and built-up category, one can note the discrepancy in dry cropland and pasture categories. Another difference is found in the irrigated cropland and pasture, which is in the Corine Land Cover situated in the southern part of the domain. This corresponds with the rice paddies found in that area. Also the fraction of water bodies in the two data sets is not similar. The Ticino river is clearly visible in the 30" USGS (lower left corner, between 45.6 latitude and 8.7 longitude and 45.3 latitude and 8.9 longitude) whereas the Ticino river is classified as "barren or sparsely vegetated" (category 19) in the Corine Land Cover data set (not shown). In Table 1b the number of cells of each land-use type in each data set is presented. Large differences are found in land-use type e.g. urban and built-up land; the urban and built-up land coverage in the Corine Land Cover data set is ~17 times larger than in 30" USGS data set. In Table 1c the type of land-use classification for each station used in the work in the USGS and Corine Land Cover is presented. For 13 (out of 22 stations) the type of land-use classification is different between USGS and Corine Land Cover.

3. Results

For the evaluation of the simulated meteorological parameters (wind speed, temperature and precipitation) we select those stations for which observations of the ARPA network are available. For the statistical analysis of simulated temperature profiles we use 20 stations, for wind speed eight stations and for precipitation 17 stations. The simulated statistics are bias, root mean square error (RMSE), standard deviation of the error (STDERR), standard deviation (SDEV) and the temporal squared correlation coefficient (R^2). For the precipitation data the statistical analysis and the sums of observed and modelled amount of precipitation were evaluated for January–February only. The capability of capturing the precipitation events by the model was evaluated using the following hit rate statistics: probability of detection (POD), false alarm (FA), frequency BIAS (FBI), Hansen–Kuipers score (HKS) and odds ratio (OR) (Stephenson, 2000; Goeber and Milton, 2002). For detailed description of the equations used to calculate statistics see Appendix A.

3.1. Wind speed

Clear differences in the average simulated wind speeds at ten metres (10 m) height between WRF_CLCW and WRF_30sW are observed outside the city of Milan (Fig. 4A and B, respectively). Large areas in WRF_CLCW, which are classified as urban areas in the Corine Land Cover data, show lower wind speeds (on average between 0.1 and 0.4 m/s lower) than WRF_30sW, while in Milan city WRF_CLCW calculates on average ~0.1 m/s higher wind speeds than WRF_30sW. The differences in average wind speeds for July–August are similar as for the winter period (lower by WRF_CLCS), see Fig. 4C and D, respectively. WRF_CLCW (and WRF_CLCS) calculates lower

Table 1c

Coordinates of the stations are given in Gauss–Boaga (a coordinate system often used in Italy), together with the longitude and latitude. In the last two columns the type of classification for the station in the USGS and Corine Land Cover is presented.

Station name	North Gauss–Boaga	East Gauss–Boaga	Lon	Lat	Classification in USGS Land Cover	Classification in Corine Land Cover
Cinisello Balsamo	5,043,277	1,516,078	9.21	45.54	Dryland cropland and pasture	Urban and built-up land
Carate Brianza	5,057,656	1,518,299	9.23	45.67	Irrigated cropland and pasture	Urban and built-up land
Milan Brera	5,035,385	1,514,809	9.19	45.47	Urban and built-up land	Urban and built-up land
Mariano Comense	5,059,985	1,514,183	9.18	45.69	Cropland/woodland mosaic	Urban and built-up land
Milan Piazza Zavattari	5,035,867	1,511,109	9.14	45.47	Urban and built-up land	Urban and built-up land
Milan Lambrate	5,038,191	1,520,147	9.26	45.50	Urban and built-up land	Urban and built-up land
Milan Viale Marche	5,038,125	1,514,945	9.19	45.50	Urban and built-up land	Urban and built-up land
Milan Viale Feltre	5,037,617	1,519,463	9.24	45.49	Urban and built-up land	Urban and built-up land
Arconate	5,043,918	1,488,109	8.85	45.55	Irrigated cropland and pasture	Dryland cropland and pasture
Rodano	5,035,531	1,527,658	9.35	45.47	Dryland cropland and pasture	Dryland cropland and pasture
Busto Arsizio Viale Magenta	5,050,830	1,488,340	8.85	45.61	Urban and built-up land	Urban and built-up land
Busto Arsizio Viale Rossini	5,052,573	1,486,298	8.82	45.62	Dryland cropland and pasture	Dryland cropland and pasture
Casatenovo	5,061,000	1,524,093	9.31	45.70	Dryland cropland and pasture	Urban and built-up land
Como Villa Gallia	5,073,520	1,505,230	9.06	45.81	Dryland cropland and pasture	Cropland/woodland mosaic
Como Villa Geno	5,074,100	1,506,234	9.08	45.82	Irrigated cropland and pasture	Urban and built-up land
Cantu Asnago	5,062,800	1,507,838	9.10	45.72	Dryland cropland and pasture	Urban and built-up land
Caslino d'Erba	5,075,805	1,518,073	9.23	45.84	Dryland cropland and pasture	Deciduous broadleaf forest
Cavaria	5,059,587	1,485,053	8.81	45.69	Urban and built-up land	Urban and built-up land
Olgiate Comasco	5,071,552	1,498,446	8.98	45.80	Dryland cropland and pasture	Urban and built-up land
Castronno	5,066,166	1,486,085	8.82	45.75	Dryland cropland and pasture	Urban and built-up land
Lurago Marinone	5,061,887	1,497,877	8.97	45.71	Deciduous broadleaf forest	Mixed forest
Paderno Dugnano	5,047,728	1,512,429	9.16	45.58	Dryland cropland and pasture	Urban and built-up land

Wind speed.

wind speeds than WRF_30sW (and WRF_30sS) since the Corine Land Cover includes more urban area in the model domain than the 30-arc second USGS data (Fig. 3) and therefore reduces the wind speed due to more friction.

The simulated wind speed values are compared with observations from eight monitoring stations, for which wind observation data is available, i.e. Cinisello Balsamo, Milan Piazza Zavattari, Milan Viale Marche, Carate Brianza, Busto

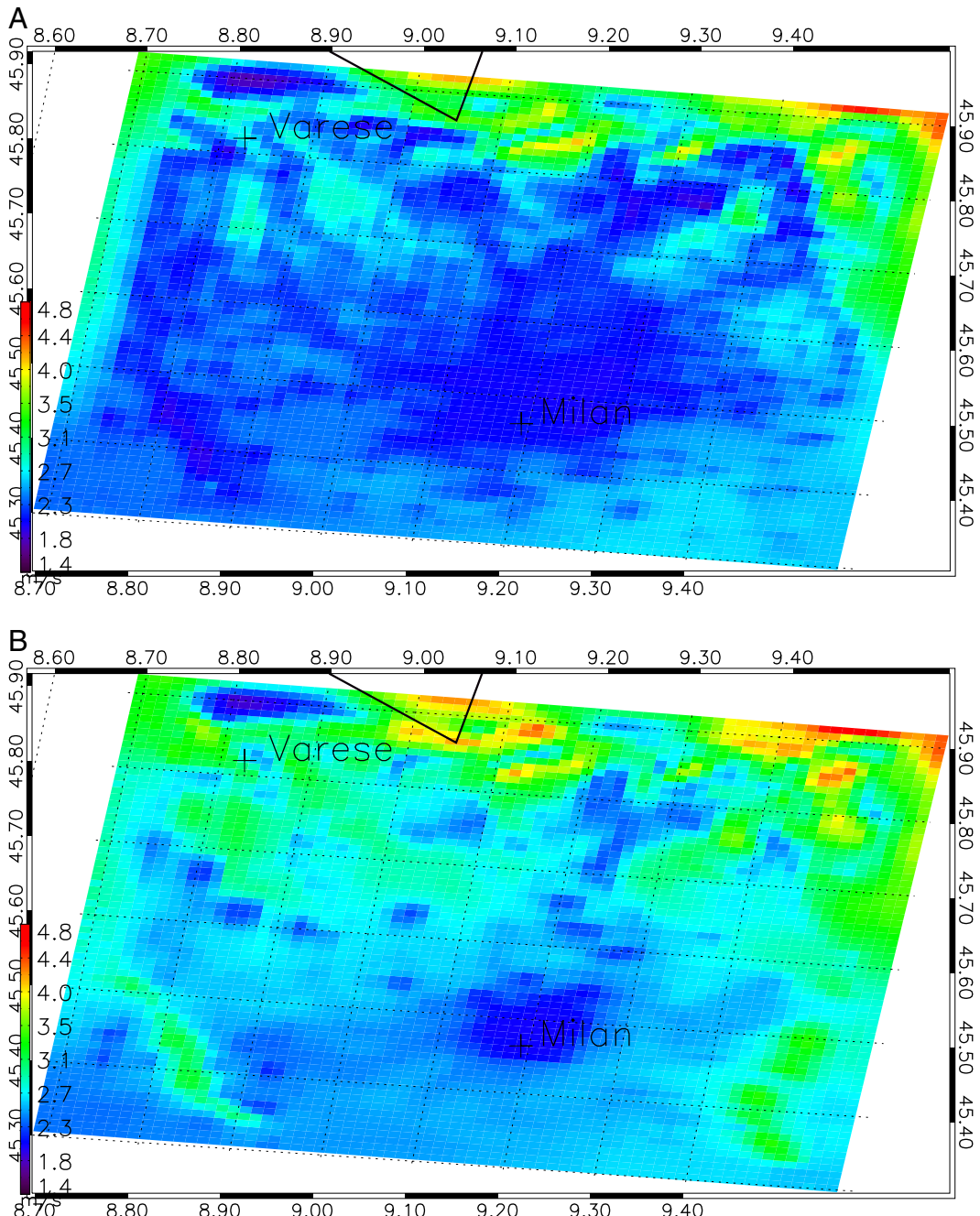


Fig. 4. Average wind speed (m/s) simulated by WRF_CLCW (A) and WRF_30sW (B) for the period January–February 2008 and for the period July–August 2008 by WRF_CLCS (C) and WRF_30SS (D). The city centres of Milan and Varese are highlighted by a plus symbol. (E) Temporal profile of the observed wind speed for Carate Brianza (black line) together with the simulated wind speed by WRF with Corine Land Cover (blue line) and WRF with USGS Land Cover (red line). (F) Scatter plot of observed wind speeds versus WRF with Corine Land Cover and (G) scatter plot of observed wind speeds versus WRF with USGS Land Cover. For reference, the 2:1 and 1:2 lines are shown as the dashed red lines, the 1:1 line as solid light blue and the line of best fit is dark blue solid.

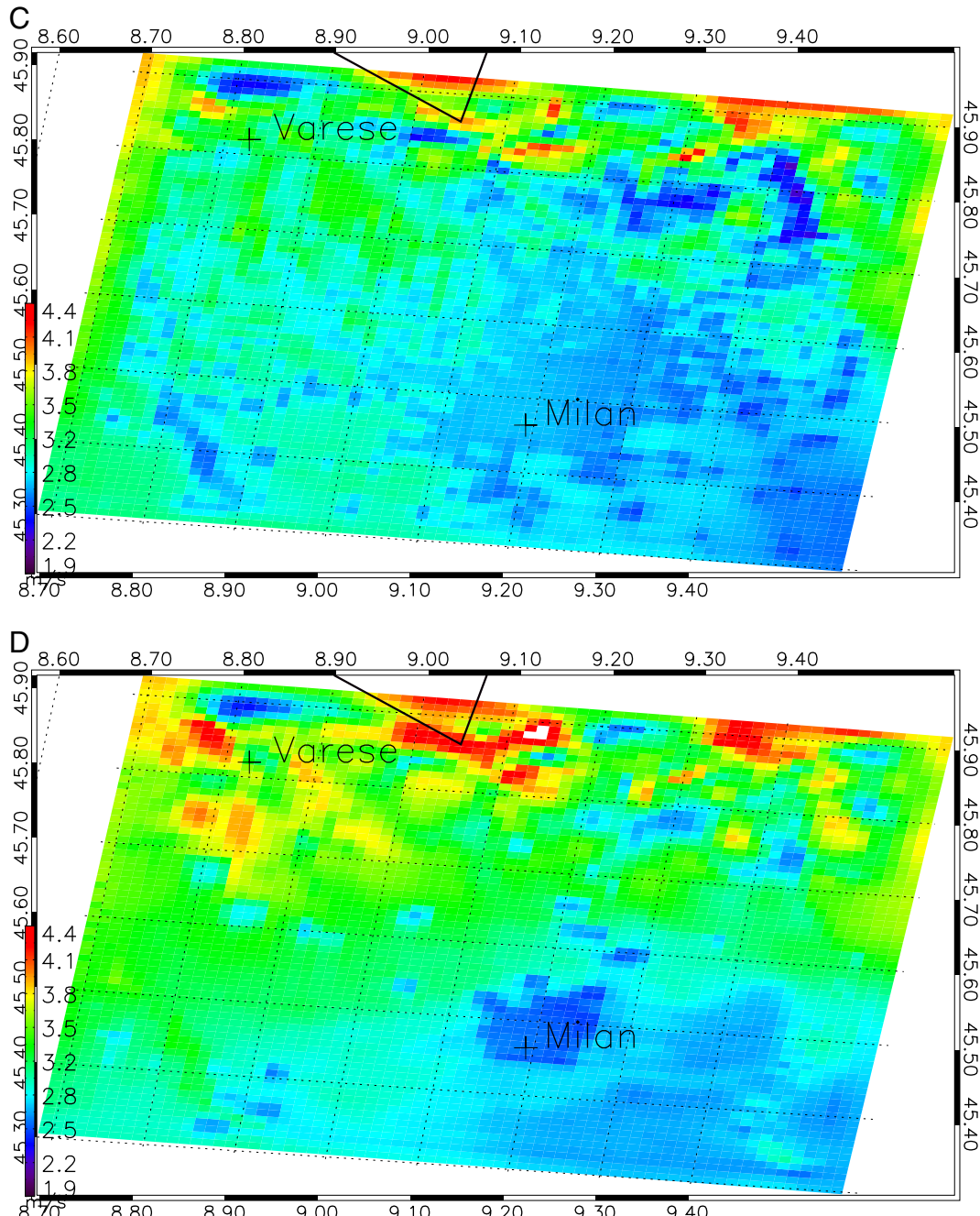


Fig. 4 (continued).

Arsizio Viale Magenta, Milan Brera, Mariano Comense and Rodano. The coordinates and type of land-use classification for these stations are given in Table 1c.

Comparing the modelled values with observations we see that WRF_CLCW and WRF_30sW overestimate the observed wind speeds. However, in general the bias of the average wind speed by WRF_CLCW is lower (0.70 m/s) than by WRF_30sW (0.78 m/s) when compared to the observations, see Table 2a. The STDERR values are on average lower by WRF_CLCW than by WRF_30sW (1.30 and 1.38, respectively).

Average wind speeds are 5% lower by WRF_CLCW (1.78 m/s) than WRF_30s (1.86 m/s), with a maximum difference of 22% for Carate Brianza (WRF_CLCW being lower; Table 1Sa–b of the Electronic Supplement). In Fig. 4E–G we show the wind speed profiles for Carate Brianza. We see clearly that both the models overestimate the wind speed, but less by the WRF_CLCW. In Table 1c we see that the Land Use category for Carate Brianza is different between USGS (Irrigated Cropland and Pasture) and Corine Land Cover (Urban and Built-up Land), which explains the lower simulated wind speed by WRF_CLCW.

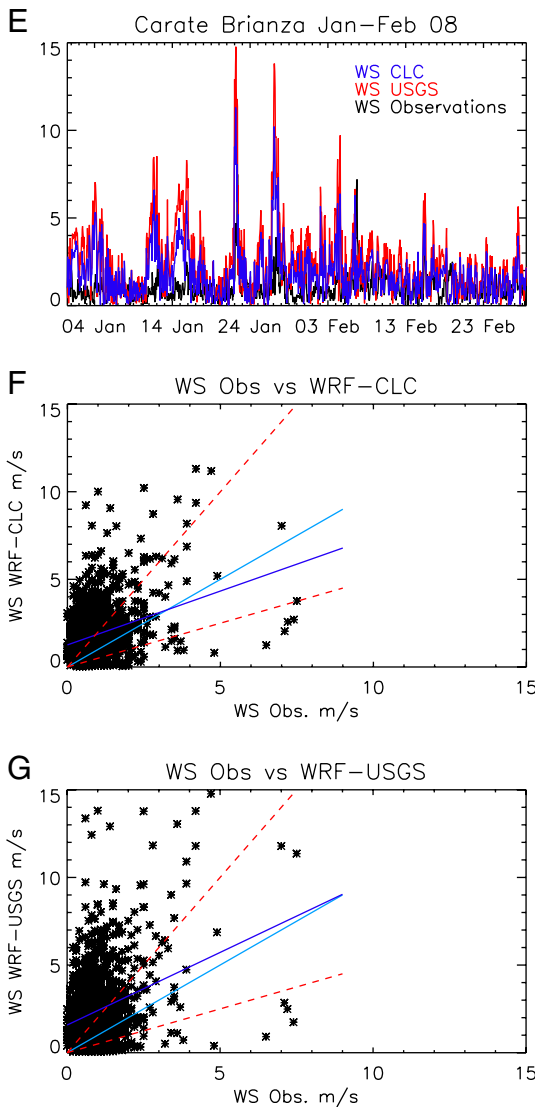


Fig. 4 (continued).

For all the stations the average wind speed by WRF_30sW is higher than WRF_CLCW (Table 2b). Maximum wind speeds are in general higher for 5 (out of 8) stations by WRF_30sW than WRF_CLCW. RMSE values vary between 1.26–1.82 m/s by WRF_CLCW and 1.24–2.37 m/s by WRF_30sW; all RMSE values are higher than the standard deviation of observed wind speeds. R^2 values are low (~0.14), which corroborates the results of De Meij et al. (2009a).

The analysis of the wind speeds for July and August shows that the maximum wind speeds are on average ~10% higher by WRF_30sS (13.39 m/s) than WRF_CLCS (12.15 m/s), and more than a factor of 2 higher than the observations (average maximum is 5.58 m/s), see Table 2c. For 6 (out of 8) stations WRF_30sS shows higher maximum wind speeds than WRF_CLCS (Table S1c–d). Average wind speeds by WRF_CLCS (2.53 m/s) are 4% lower than the average wind speeds by WRF_30sS (2.64 m/s), with a maximum difference of 20% for Carate Brianza and 22% for Mariano Comense (WRF_CLCS

being lower than WRF_30sS). In general the bias of the average wind speeds by WRF_CLCS is lower (1.21) than by WRF_30sS (1.32), indicating that the overestimation of the observations is less than by WRF_CLCS (Table 2d). The STDERR values are on average lower by WRF_CLCS than by WRF_30sS (1.43 and 1.55, respectively). The RMSE values are in general higher than the standard deviation of the observed wind speeds. R^2 values are low (~0.08).

3.2. Temperature

With respect to the average simulated temperature at 2 m clear differences are found outside the city of Milan between WRF_CLCW and WRF_30sW (Fig. 5A and B, respectively). In the areas for which the USGS data set does not register urban and built-up areas, the differences between WRF_CLCW and WRF_30sW vary between ~0.2 and ~1.0 degrees Celsius ($^{\circ}$ C) and ~1.2 $^{\circ}$ C for Milan. Higher temperatures may deepen the PBL heights, which lead to a better mixing of the air pollutants in the first vertical layers. Nevertheless, a change in surface temperature may affect e.g. the emission rates of biogenic and anthropogenic emissions and volatility of aerosols, which could also affect the air pollutant concentrations in the first layers. However, the impact of the temperature on gas and aerosol pollutants is beyond the scope of this paper.

To understand better the differences in simulated temperatures at 2 m between WRF_CLSW and WRF_30sW we analyse in Fig. 5C–H the upward sensible and latent heat fluxes and PBL heights by the two simulations. The sensible (dry) and latent (moist) heat fluxes determine the growth of the PBL. When the ratio between sensible and latent heat fluxes (Bowen ratio) is large (sensible heat flux > latent heat flux) the PBL is deeper than when the Bowen ratio is small (e.g. 0.5 over wet areas). Over most land surfaces the sensible heat fluxes determine the convection of air in the atmosphere (Ball, 1960) and therefore the PBL. When the latent heat fluxes are higher than the sensible heat fluxes, the temperature near the surface is lower compared to the areas where the sensible heat fluxes and PBL heights are higher (Fraedrich et al., 1999).

In Fig. 5C–D, the mean sensible heat fluxes between January and February 2008 are shown by WRF_CLCW and WRF_30sW, respectively. The sensible heat fluxes by WRF_CLCW are in general higher for a large area in the domain than by WRF_30sW. The higher values of sensible heat fluxes in WRF_CLCW correspond to the location of the urban built-up area in the Corine Land Cover. Table 1b shows that a larger area in WRF_CLCW is classified as urban area than as in WRF_30sW (~17 times more as mentioned earlier). Larger sensible heat fluxes result in larger PBL heights (Van den Hurk, 1995) as shown in Fig. 5E–F. In a large part of the model domain the PBL heights are higher by WRF_CLCW than by WRF_30sW due to the higher values of the sensible heat fluxes by WRF_CLCW, as mentioned before. In Fig. 5G–H, the mean latent heat fluxes between January–February 2008 by WRF_CLCW and WRF_30sW are presented. Clearly the differences in latent heat fluxes are present between WRF_CLCW and WRF_30sW. Higher latent heat fluxes by WRF_30sW result in lower temperature profiles at the surface as shown in Fig. 5A and B. For the summer period the differences in average temperatures are larger up to

Table 2a

Average wind speed statistics based on 8 stations for January–February 2008 by the WRF simulation with Corine Land Cover (WRF_CLCW) and the simulation with 30-arc second USGS Land Cover (WRF_30sW). Bias, Standard deviation (STDEV) and Standard Deviation Error (STDERR) are in m/s. The statistics for each station can be found in the Electronic Supplement.

January–February 2008											
Wind speed	WRF_CLCW	WRF_30sW	WRF_CLCW	WRF_30sW	WRF_CLCW	WRF_30sW	Obs	WRF_CLCW	WRF_30sW	WRF_CLCW	WRF_30sW
	BIAS	BIAS	RMSE	RMSE	STDERR	STDERR	STDEV	STDEV	STDEV	R ²	R ²
Average	0.71	0.78	1.52	1.64	1.30	1.38	0.73	1.38	1.48	0.14	0.14

2.7 °C, while for Milan the differences are around 0.7 °C (Fig. 5I–J). Similar differences in sensible and latent heat fluxes between the simulation with SRTM–Corine Land Cover and the USGS data sets are found for the summer period (not shown) as for the winter period.

In this paragraph we compare the simulated temperatures with the observations. Analyzing the simulated temperatures with observations for the period January–February 2008, we see that R² values by WRF_CLCW are on average a factor of 1.03 higher than by WRF_30sW, with a maximum of 14% for the Como Villa Gallia station (Table S1e). The calculated biases show for seven (out of 20) stations that WRF_30sW underestimates the observed temperatures, while WRF_CLCW underestimates for four stations the observed values. The average bias in Table 2e by WRF_30sW (0.48) is lower than by WRF_CLCW (0.97) and the STDERR values are on average lower by WRF_CLCW than by WRF_30sW (2.34 and 2.42, respectively). In all cases (except for Arconate station) the relation RMSE_{mod} < STDEV_{obs} is valid, which is one of the conditions for good quality modelling results (Barna and Lamb, 2000). The maximum temperatures are better represented by WRF_CLCW (Tables 2f and S1f), while the average minimum temperatures for both WRF_CLCW and WRF_30sW are too high (−2.2 °C and −2.6 °C, respectively) when compared to the observations (−4.47 °C). In Fig. 5 k we show the temperature profiles for Carate Brianza for January–February. This station is classified in the Corine Land Cover as Urban and Built-up Land and as Irrigated Cropland and Pasture in the USGS data set. We see clearly that both simulations overestimate in general the minimum temperatures and underestimate the maximum temperatures when compared to the observations. In general higher minimum and maximum temperatures are simulated by WRF_CLCW than by WRF_30sW, which are related to the difference in Land Cover and the resulting differences in heat fluxes. The temporal squared correlation coefficients are 0.72 and 0.65 by WRF_CLCW and WRF_30sW, respectively. Analyzing the sensible and latent heat fluxes helps to understand the differences in temperature between the two simulations. The average sensible and latent heat fluxes by WRF_CLCW are 18.0 W/m² and 1.13 W/m², respectively and by WRF_30sW 5.91 W/m² and 16.7 W/m², respectively. Minimum and

maximum sensible heat fluxes are −172.7 W/m² and 211.3 W/m² by WRF_CLCW and −223.5 W/m² and 178.8 W/m² by WRF_30sW, respectively. Minimum and maximum latent heat fluxes are −14.0 W/m² and 27.9 W/m² by WRF_CLCW and −10.9 W/m² and −198.4 W/m² by WRF_30sW, respectively. These differences in the sensible and latent heat fluxes explain the differences in temperatures due to the differences in Land Cover as mentioned earlier. For July–August the R² values by WRF_CLCS are on average a factor of 1.14 higher than R² values by WRF_30sS, with a maximum of 1.38 for Milan Lambrate (Table S1g). The average bias by WRF_30sS is lower than by WRF_CLCS (Table 2g). Biases by WRF_30sS show that the simulation underestimates for five stations the observed temperatures, while by WRF_CLCS the temperatures are underestimated for two stations. The STDERR values are on average lower by WRF_CLCS than by WRF_30sS (2.88 and 3.27, respectively). In all cases (except for Milan Lambrate station) the relation RMSE_{mod} < STDEV_{obs} is valid. The minimum temperatures are in general overestimated by WRF_CLCS by 16%, while WRF_30sS in general underestimates the minimum temperatures by ~2.4% (Table 2h). The difference between the minimum temperature by WRF_CLCS and WRF_30sS is on average 19%. Maximum temperatures are in good agreement with the observations for both WRF_CLCS (in general overestimated by 1%) and WRF_30sS (in general underestimated by 1%).

3.3. Precipitation

In this section we analyse the statistics for the precipitation. In-cloud and below cloud wet scavenging (precipitation) are one of the most important removal mechanisms of gas and aerosol pollutants. These mechanisms determine the lifetime of the aerosols, which are size and location dependent. Below cloud scavenging is linked to aerosol concentration and size distribution and precipitation intensity (De Meij, 2009b).

The analysis of the hit rate statistics for precipitation events for the period January–February 2008 was performed using five threshold values for the precipitation amount accumulated over the day: 0.1 mm/day, 0.2 mm/day, 0.5 mm/day, 1 mm/day, and 2 mm/day. The selected threshold values describe the amount

Table 2b

Average wind speed statistics based on 8 stations for January–February 2008 by the WRF simulation with Corine Land Cover (WRF_CLCW) and the simulation with 30-arc second USGS Land Cover (WRF_30sW). Minimum, maximum and mean values are in m/s. The statistics for each station can be found in the Electronic Supplement.

Wind speed	Min	Min	Min	Max	Max	Max	Mean	Mean	Mean
	Obs	WRF_CLCW	WRF_30sW	Obs	WRF_CLCW	WRF_30sW	Obs	WRF_CLCW	WRF_30sW
Average	0.08	0.02	0.02	5.83	10.10	11.12	1.08	1.78	1.86

Table 2c

Average wind speed statistics based on 8 stations for July–August 2008 by the WRF simulation with Corine Land Cover (WRF_30sS) and the simulation with 30-arc second USGS Land Cover (WRF_30sS). Minimum, maximum and mean values are in m/s. The statistics for each station can be found in the Electronic Supplement.

Wind speed	Min	Min	Min	Max	Max	Max	Mean	Mean	Mean
	Obs	WRF_CLCS	WRF_30sS	Obs	WRF_CLCS	WRF_30sS	Obs	WRF_CLCS	WRF_30sS
Average	0.08	0.09	0.05	5.58	12.15	13.39	1.36	2.53	2.64

of precipitation in different bins for that region and for which the hit rate statistics still give reasonable values. We decided to analyse the hit rate statistics only for the winter period (January–February), because the number of precipitation events differs between the winter and the summer periods. During the winter period the number of precipitation events is ~176, while during the summer the number of precipitation events is ~42 (a factor of ~4 lower). This low number of precipitation events would make our analysis not statistically robust.

The probability of detection of the precipitation event (POD) parameter is in general 1% higher by WRF_CLCW than by WRF_30sW (Table 2i). For the lower threshold values (0.1 mm, 0.2 mm and 0.5 mm) WRF_CLCW shows an increase in POD of ~0.5%. For threshold values 1 mm and 2 mm WRF_CLCW shows an increase in POD of 1.6% and 1.4%, respectively (Table S1i). The false alarm (FA) values, which represent the probability of false detection of the rain event, are in general similar (not shown). For some stations a marginal improvement of the FA is found by WRF_CLCW (<~0.5%). The frequency bias (FBI) is that statistical measure of over- or underestimation of the number of (precipitation) events; FBI = 1 indicates that the event is forecasted exactly as often as it is observed. The average FBI (Table 2j) is similar between the two simulations for all the threshold values, except for threshold value 2 mm (WRF_CLCW is 4% lower than WRF_30sW). For the threshold value 0.1 mm the number of precipitation events is underestimated by both WRF_CLCW and WRF_30sW (FBI <1) for Rodano, Milan Piazza Zavattari, Milan Lambrate, Paderno Dugnano, Carate Brianza and Canu Asnago (Table S1j). The FBI for 0.2 mm is for 5 stations (out of 17) lower than 1. The FBI for 0.5 mm and 1 mm are larger than 1, which means that both WRF_CLCW and WRF_30sW overestimate the number of precipitation events. For the threshold value 2 mm for all the stations the number of precipitation events is overestimated by both WRF_CLCW and WRF_30sW. Interesting is that for the threshold value 2 mm for the stations located close to mountains ~1000 m, i.e. Como Villa Geno, Como Villa Gallia and Caslino d'Erba lower values of

the FBI are found by WRF_CLCW, which is probably to the implementation of the higher resolution of SRTM topography (~90), which leads to better timing of the precipitation events.

The Hansen–Kuipers score (HKS), which summarizes the model's ability to correctly time both the precipitation events and to avoid the false alarms, is in general higher by WRF_CLCW; on average 1% for all the threshold values (Table 2k). For the lower threshold values (0.1 mm, 0.2 mm and 0.5 mm) WRF_CLCW shows an increase in HKS of ~0.3%. For 0.1 mm, the HKS by WRF_CLCW is higher than WRF_30sW for eleven (out of 17) stations (Table S1k). For the threshold value 0.2 mm, the HKS by WRF_CLCW is higher than WRF_30sW by ten (out of 17) stations and for the threshold value 0.5 mm the HKS by WRF_CLCW is higher than WRF_30sW by nine (out of 17) stations. For the higher threshold values (1 mm and 2 mm) an increase in the HKS of 1.8% and 1.9% is found, respectively (WRF_CLCW higher). For the threshold value 1 mm, the HKS is for 12 (out of 17) stations higher by WRF_CLCW than by WRF_30sW and for the threshold value 2 mm the HKS by WRF_CLCW is higher for 14 stations (out of 17) than by WRF_30sW.

The Odds Ratio (OR) is greater than one in all cases for both WRF_CLCW and WRF_30sW (not shown), which indicates high HR/FA ratio; OR > 1 indicates that the probability of detection (POD) is greater than the False Alarm (FA). The analysis of the total amount of rain observed between January and February 2008 and simulated by WRF_CLCW and WRF_30sW shows that both simulations overestimate the amount of measured precipitation by a factor of 1.28 and 1.29 respectively.

The improvement of precipitation using the Corine Land Cover is likely to be related to the differences in latent and sensible heat fluxes, which affect the cloud water mixing ratio and therefore the cloud formation and the resulting precipitation.

4. Conclusions

We evaluated the impact of using the high resolution ~90 m SRTM topography together with the 100 × 100 m

Table 2d

Average wind speed statistics based on 8 stations for July–August 2008 by the WRF simulation with Corine Land Cover (WRF_30sS) and the simulation with 30-arc second USGS Land Cover (WRF_30sS). Bias, Standard deviation (STDEV) and Standard Deviation Error (STDERR) are in m/s. The statistics for each station can be found in the Electronic Supplement.

July–August 2008											
Wind speed	WRF_CLCS	WRF_30sS	WRF_CLCS	WRF_30sS	WRF_CLCS	WRF_30sS	Obs	WRF_CLCS	WRF_30sS	WRF_CLCS	WRF_30sS
BIAS	BIAS	RMSE	RMSE	STDERR	STDERR	STDEV	STDEV	STDEV	STDEV	R ²	R ²
Average	1.21	1.32	1.82	1.98	1.43	1.55	0.72	1.55	1.69	0.08	0.08

Corine Land Cover data on the simulated meteorological variables wind speed at 10 m height, temperature at 2 m and precipitation in WRF by comparing with the simulation using the standard 30" ($\sim 1 \times 1$ km) USGS Land Cover and

with observations of the ARPA network for the periods January–February and July–August 2008.

Our analysis indicates that between January and February 2008 lower average wind speeds are simulated by WRF with

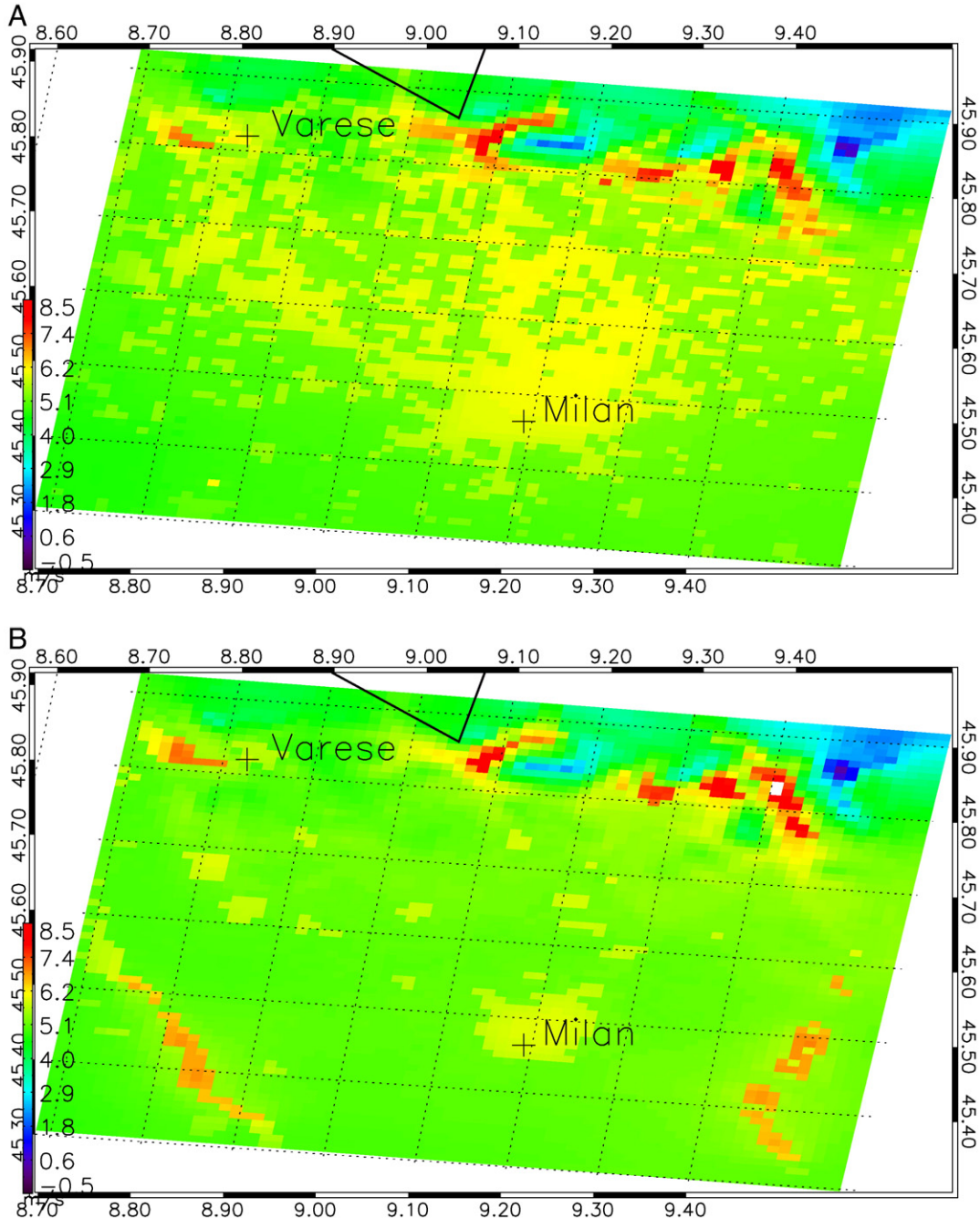
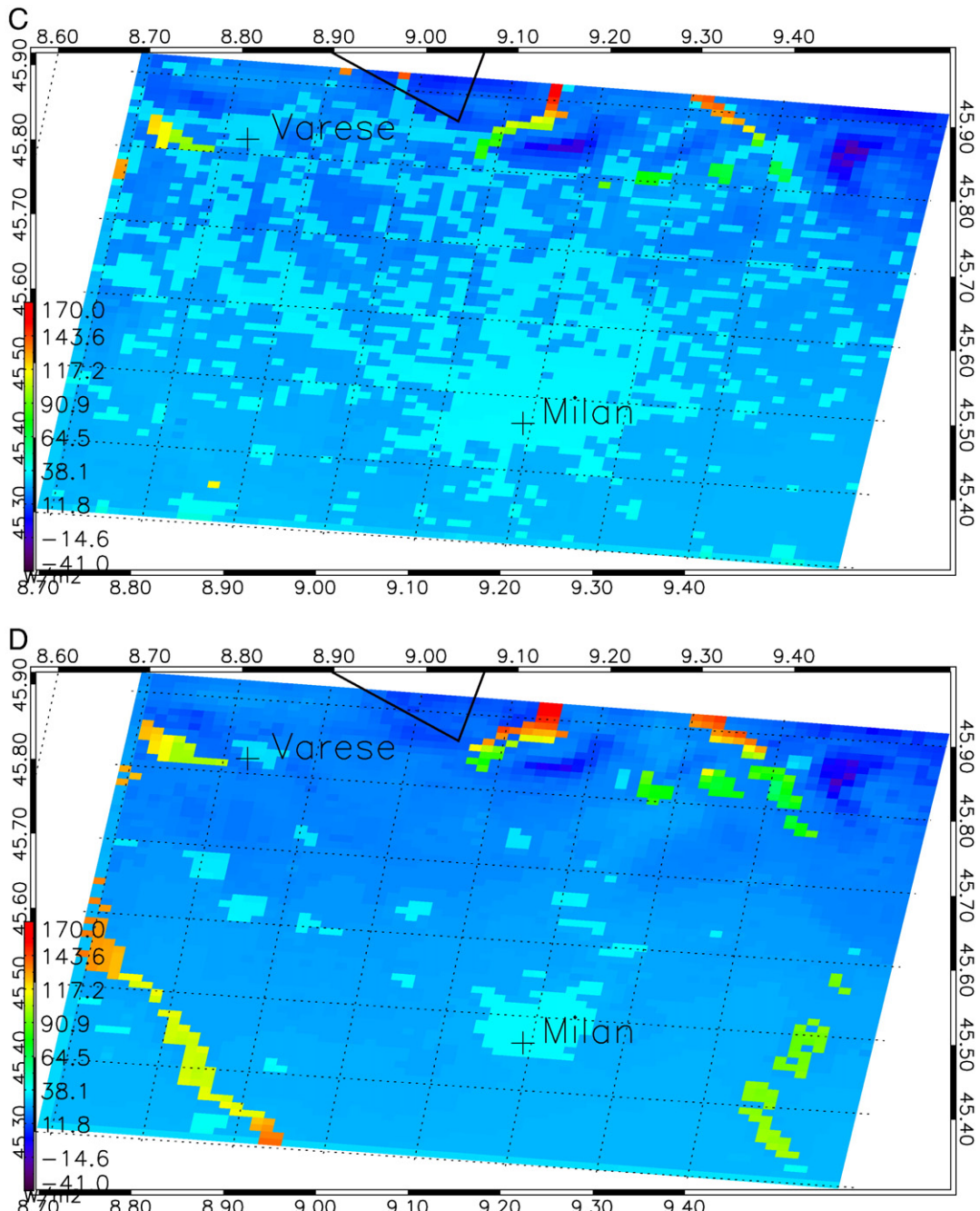


Fig. 5. Average temperatures at 2 m height ($^{\circ}\text{C}$) simulated by WRF_CLCW (A) and WRF_30sW (B) for the period January–February 2008. The city centres of Varese and Milan are highlighted by a plus symbol. The white pixel in Mean T2 Jan–Feb 30s represents the maximum value of $8.6 ^{\circ}\text{C}$. C–D. Mean sensible heat flux (W/m^2) between January and February 2008 by WRF_CLCW (C) and WRF_30sW (D). E–F. Mean PBL heights (m) between January and February 2008 by WRF_CLCW (E) and WRF_30sW (F). G–H. Mean latent heat flux (W/m^2) between January and February 2008 by WRF_CLCW (g) and WRF_30sW (H). The white pixels represent latent heat fluxes larger than 70 W/m^2 . I–J. Average temperatures at 2 m height ($^{\circ}\text{C}$) for the period July–August 2008 by WRF_CLCS (I) and WRF_30sS (J). The city centres of Varese and Milan are highlighted by a plus symbol. k. Measurements of the temperature profile for Cinesello Balsamo together with simulated temperatures by WRF with Corine Land Cover and WRF with USGS. Temperatures are in degrees Celsius.

**Fig. 5 (continued).**

the SRTM and Corine Land Cover than with 30" USGS. The reason for this is that the urban and built-up land coverage in the Corine Land Cover data set is ~17 times larger than in 30" USGS data set. A higher fraction of urban and built-up land cover results in more friction and higher roughness in the domain, which lowers the wind speeds at ground level. The differences in average simulated wind speeds between the two simulations are smaller for July–August. Comparing the simulated wind speeds with observations shows that the wind speeds are in general overestimated (less by WRF with

Corine Land Cover). The biases for the simulation with the SRTM and Corine Land Cover are lower for the both periods (January–February and July–August) than the simulation with the 30" USGS.

Clear differences are found in simulated temperature at 2 m height between the two simulations outside the city of Milan for the winter and summer periods. The reason for this is that the higher fraction of urban and built-up area in the Corine Land Cover impacts the simulated sensible and latent heat fluxes. The simulation with the Corine Land Cover

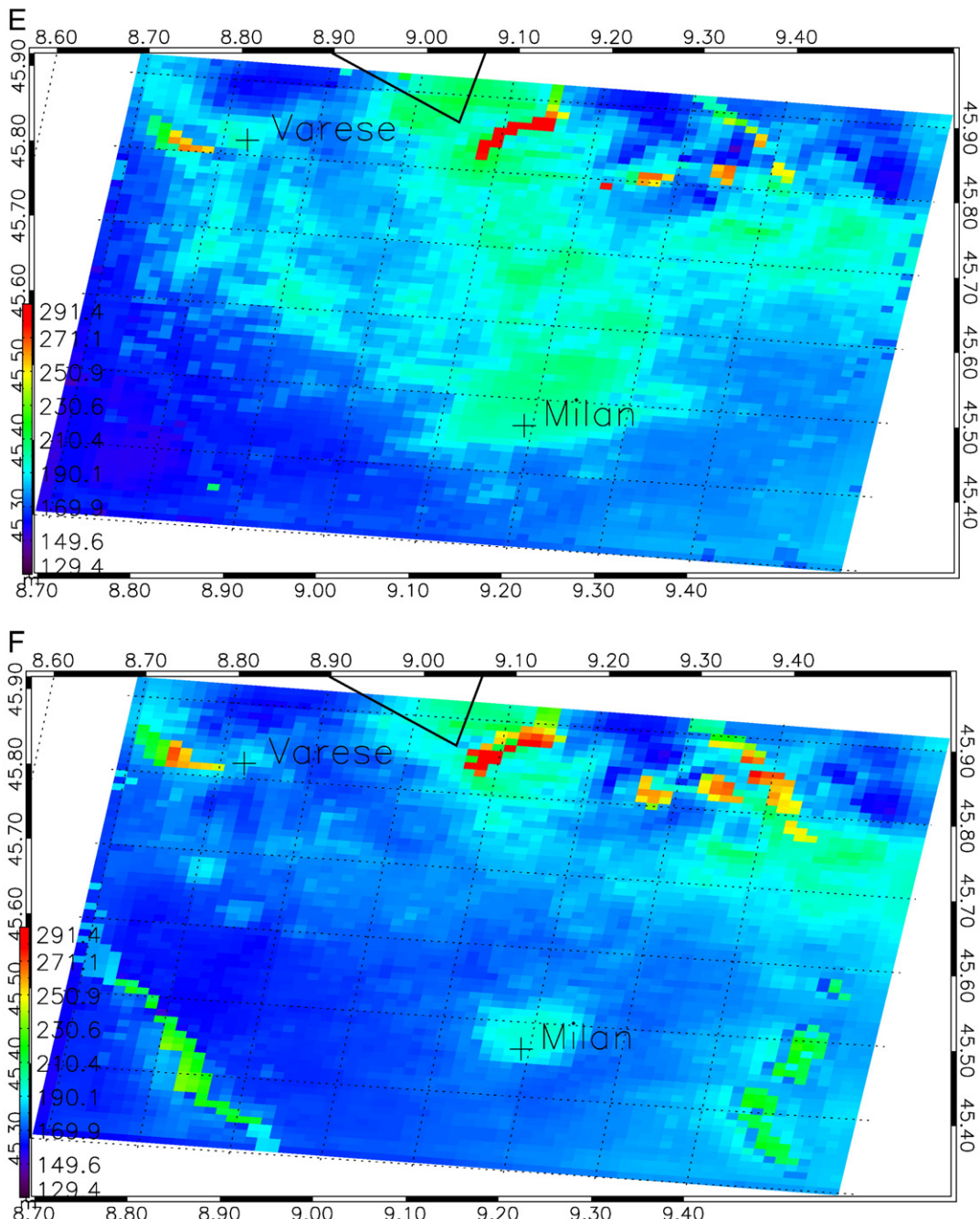


Fig. 5 (continued).

simulates in general higher sensible heat fluxes for a large area in the domain (which corresponds with the location of the urban built-up area) than the simulation with the USGS Land Cover. The latent heat fluxes are higher by the simulation with the USGS Land Cover, which lowers the surface temperatures. The urban and built-up area holds the heat between the buildings, which causes the urban areas to be warmer than the surrounding rural areas. The average bias for WRF with the USGS data set is lower than for the simulation with the SRTM and Corine Land Cover. R^2 values

for the simulation with the SRTM and Corine Land Cover are on average a factor of 1.03 higher than the simulation with the USGS data set. For the period July–August the R^2 values for the simulation with the SRTM and Corine Land Cover are on average 1.14 higher. Biases show that in general WRF with SRTM and Corine Land Cover overestimates the temperatures, while WRF with 30" USGS underestimates for five stations the observed temperatures. The differences in simulated temperature profiles by the two simulations during the winter and summer periods are related to the differences in sensible and

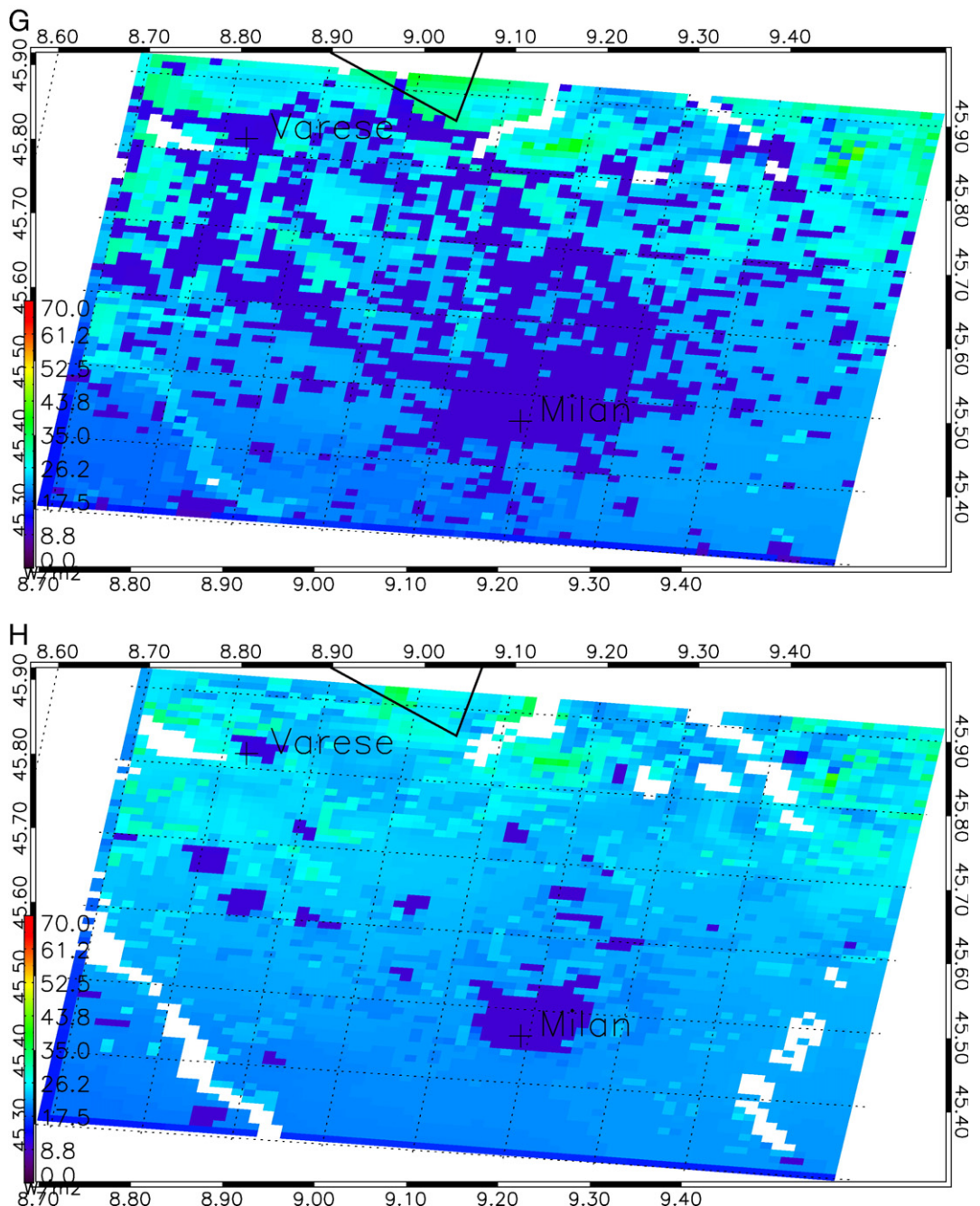


Fig. 5 (continued).

latent heat fluxes and the related PBL heights. Maximum temperatures are in good agreement with the observations for both the simulations. In almost all cases the relation $\text{RMSE}_{\text{mod}} < \text{STDEV}_{\text{obs}}$ is valid.

The probability of detection of the precipitation event is somewhat higher (on average 1%) by the simulation with the SRTM and Corine Land Cover than simulation with 30" USGS, while the false alarm values are in general similar. The

frequency bias for the threshold values 0.5 mm and 1.0 mm is for both the simulations larger than 1, indicating that the simulations overestimate the number of precipitation events for these thresholds. For the threshold value 2 mm the models overestimate the number of precipitation events. The Hansen-Kuipers score, which summarizes the model's ability to correctly time both the precipitation events and to avoid the false alarms, is in general 1% higher for WRF with SRTM

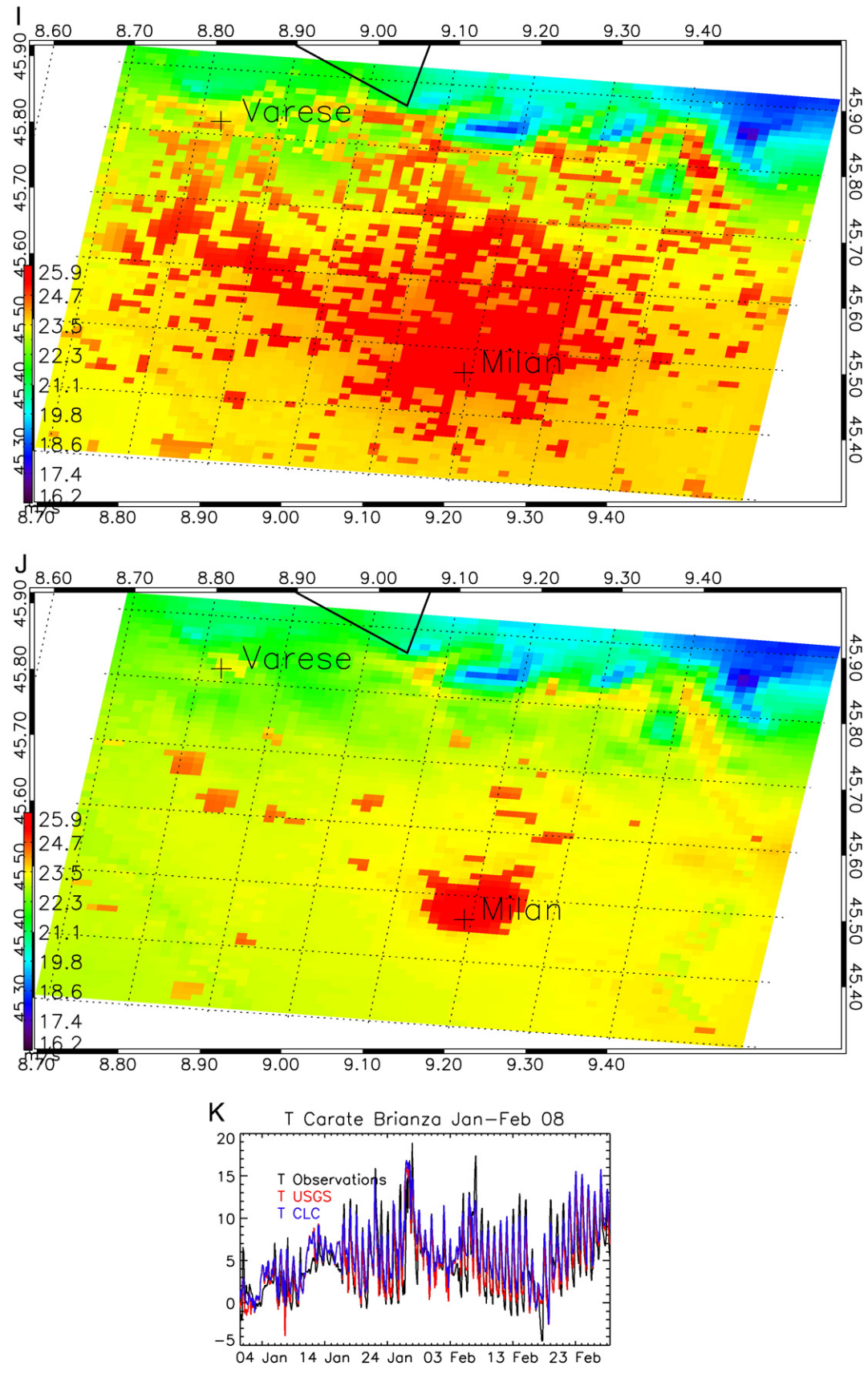


Fig. 5 (continued).

Table 2e

Average temperature statistics based on 20 stations for January–February 2008 by the WRF simulation with Corine Land Cover (WRF_CLCW) and the simulation with 30-arc second USGS Land Cover (WRF_30sW). Bias, Standard deviation (STDEV) and Standard Deviation Error (STDERR) are in °C. The statistics for each station can be found in the Electronic Supplement.

January–February 2008											
Temperature	WRF_CLCW	WRF_30sW	WRF_CLCW	WRF_30sW	WRF_CLCW	WRF_30sW	Obs	WRF_CLCW	WRF_30sW	WRF_CLCW	WRF_30sW
BIAS	BIAS	RMSE	RMSE	STDERR	STDERR	STDERR	STDEV	STDEV	STDEV	R ²	R ²
Average	0.97	0.48	2.71	2.64	2.34	2.42	3.98	3.58	3.56	0.68	0.66

Table 2f

Average temperature statistics based on 20 stations for January–February 2008 by the WRF simulation with Corine Land Cover (WRF_CLCW) and the simulation with 30-arc second USGS Land Cover (WRF_30sW). Minimum, maximum and mean values are in °C. The statistics for each station can be found in the Electronic Supplement.

January–February 2008								
Temperature	Min Obs	Min WRF_CLCW	Min WRF_30sW	Max Obs	Max WRF_CLCW	Max WRF_30sW	Mean Obs	Mean WRF_CLCW
Average	–4.47	–2.20	–2.60	18.81	16.88	16.63	5.09	5.84

Table 2g

Average temperature statistics based on 20 stations for July–August 2008 by the WRF simulation with Corine Land Cover (WRF_CLCS) and the simulation with 30-arc second USGS Land Cover (WRF_30sS). Bias, Standard deviation (STDEV) and Standard Deviation Error (STDERR) are in °C. The statistics for each station can be found in the Electronic Supplement.

July–August 2008											
Temperature	WRF_CLCS	WRF_30sS	WRF_CLCS	WRF_30sS	WRF_CLCS	WRF_30sS	Obs	WRF_CLCS	WRF_30sS		
BIAS	BIAS	RMSE	RMSE	STDERR	STDERR	STDERR	STDEV	STDEV	R ²		
Average	1.52	0.31	3.36	3.34	2.88	3.27	4.26	3.73	4.12	0.59	0.51

and Corine Land Cover for all the threshold values. Both simulations overestimate by a factor of ~1.28 of the total amount of observed precipitation.

Our analysis clearly shows that using high resolution topography and, in particular, land-use improves the results of calculating wind speeds, temperature and precipitation on 1 × 1 km. A host of studies showed that the underestimation of simulated PM concentrations by ACTMS is partly related to the overestimation of wind speeds by the meteorological drivers and the uncertainties in wet scavenging, as mentioned

in the [Introduction](#). Therefore, ACTMs will strongly benefit from the use of the high resolution SRTM and Corine Land Cover data, especially with regard to reducing the bias between observed and simulated aerosol (precursor) concentrations, which is necessary for scientific studies and for policy making. Besides this, environmental sustainable related projects (e.g. ENORASIS; <http://www.enorasis.eu/>) for which meteorological models are used for optimizing irrigation management by farmers will benefit from higher precision precipitation, wind speed and temperature fields by the meteorological models.

Table 2h

Average temperature statistics based on 20 stations for July–August 2008 by the WRF simulation with Corine Land Cover (WRF_CLCS) and the simulation with 30-arc second USGS Land Cover (WRF_30sS). Minimum, maximum and mean values are in °C. The statistics for each station can be found in the Electronic Supplement.

July–August 2008								
Temperature	Min Obs	Min WRF_CLCS	Min WRF_30sS	Max Obs	Max WRF_CLCS	Max WRF_30sS	Mean Obs	Mean WRF_CLCS
Average	12.71	14.80	12.40	32.89	33.23	32.64	22.90	24.28

Table 2i

Average probability of detection of precipitation based on 17 stations by the WRF simulation with Corine Land Cover (WRF_CLCW) and the simulation with 30-arc second USGS Land Cover (WRF_30W) for January–February 2008. The statistics for each station can be found in the Electronic Supplement.

January–February 2008										
Probability of Detection	0.1 mm WRF_CLCW	0.1 mm WRF_30sW	0.2 mm WRF_CLCW	0.2 mm WRF_30sW	0.5 mm WRF_CLCW	0.5 mm WRF_30sW	1 mm WRF_CLCW	1 mm WRF_30sW	2 mm WRF_CLCW	2 mm WRF_30sW
Average	0.73	0.73	0.72	0.72	0.65	0.64	0.48	0.47	0.28	0.27

Table 2j

Average frequency bias of precipitation based on 17 stations by the WRF simulation with Corine Land Cover (WRF_CLCW) and the simulation with 30-arc second USGS Land Cover (WRF_30sW) for January–February 2008. The statistics for each station can be found in the Electronic Supplement.

January–February 2008											
Threshold value:	0.1 mm	0.1 mm	0.2 mm	0.2 mm	0.5 mm	0.5 mm	1 mm	1 mm	2 mm	2 mm	
Frequency bias	WRF_CLCW	WRF_30sW									
Average	1.15	1.14	1.19	1.18	1.35	1.35	1.57	1.57	1.26	1.31	

Table 2k

Average Hansen Kuipers score of precipitation based on 17 stations by the WRF simulation with Corine Land Cover (WRF_CLCW) and the simulation with 30-arc second USGS Land Cover (WRF_30sW) for January–February 2008. The statistics for each station can be found in the Electronic Supplement.

January–February 2008											
Threshold value:	0.1 mm	0.1 mm	0.2 mm	0.2 mm	0.5 mm	0.5 mm	1 mm	1 mm	2 mm	2 mm	
Hansen Kuipers score	WRF_CLC	WRF_30s									
Average	0.69	0.68	0.68	0.68	0.60	0.59	0.43	0.43	0.26	0.26	

It is noteworthy to mention that the original resolution of the ~90 m SRTM and Corine Land Cover (100×100 m) is not the same as the model finest resolution (1×1 km) used in this study. Using the SRTM and Corine Land Cover on a much coarser resolution (e.g. 10×10 km) will probably show less difference in the land-use categories (e.g. the urban built-up area) and topography when compared to the USGS data sets. Therefore the impact of high resolution topography and land cover on the simulated meteorological parameters on grid resolutions of e.g. 10×10 km will be less prevalent.

Acknowledgements

We would like to thank ARPA Lombardia for making the meteorological observations publicly available through their website. We would also like to thank the reviewers for their constructive comments. This study is fully funded by NOVELTIS' internal R&D initiative.

Appendix A

Definition of the rain specific hit rate statistics used for the comparison between modelled and observed values.

For the hit rate statistics the following symbolic representation was used:

Based on this the following categorical statistics were simulated:

		Observation	
		Yes	No
Model	Yes	A	B
	No	C	D

A – correct hits.

B – false hits (false alarm).

C – false rejections (misses).

D – correct rejections.

Probability of detection of the rain event:

$$\text{POD} = \frac{A}{A + C}.$$

False alarm (probability of false detection of the rain event):

$$\text{FA} = \frac{B}{B + D}.$$

Frequency BIAS (the measure of over – or underestimation of the events number; FBI = 1 indicates that the event is forecasted exactly as it is observed):

$$\text{FBI} = \frac{A + C}{A + B}.$$

Hansen–Kuipers score (indicates the ability of the model to give correct forecast of the event as well as to avoid the false alarms):

$$\text{HKS} = \frac{AD - BC}{(A + C)(B + D)}.$$

Odds ratio (OR > 1 indicates that the POD > FA) (Stephenson, 2000; Goeber and Milton, 2002):

$$\text{OR} = \frac{AD}{BC}.$$

Appendix B. Supplementary data

Supplementary data to this article can be found online at <http://dx.doi.org/10.1016/j.atmosres.2014.03.004>.

References

- Anderson, et al., 1976. System for Land Use and Land Cover Classification.
- Arnold, D., Schicker, I., Seibert, P., 2010. High-resolution atmospheric modelling in complex terrain for future climate simulations (HiRmod). Vienna Scientific Cluster Report 2010 (<http://www.boku.ac.at/met/envmet/hirmod.html>).
- Ball, F.K., 1960. Control of inversion height by surface heating. Q. J. R. Meteorol. Soc. 86, 483–494.

- Barna, M., Lamb, B., 2000. Improving ozone modeling in regions of complex terrain using observational nudging in a prognostic meteorological model. *Atmos. Environ.* 34, 4889–4906.
- Büttner, G., et al., 1998. The European CORINE Land Cover Database. ISPRS Commission VII Symposium, Budapest, September 1–4, 1998. Proceedings, pp. 633–638.
- Büttner, G., Feranec, G., Jaffrain, G., 2002. Corine land cover update 2000, Technical guidelines. EEA Technical report No 89 (http://reports.eea.europa.eu/technical_report_2002_89/en).
- Carvalho, A.C., Carvalho, A., Gelpi, I., Barreiro, M., Borrego, C., Miranda, A.I., Pérez-Muñozuri, V., 2006. Influence of topography and land-use on pollutants dispersion in the Atlantic coast of Iberian Peninsula. *Atmos. Environ.* 40, 3969–3982.
- Chen, F., Dudhia, J., 2001. Coupling an advanced land surface/hydrology model with the Penn State/NCAR MM5 modeling system. Part I: model description and implementation. *Mon. Weather Rev.* 129, 569–585.
- Chou, Suarez, M.J., 1999. A solar radiation parameterization (CLIRAD-SW) developed at Goddard Climate and Radiation Branch for Atmospheric Studies. Technical Memorandum 15, Technical Report Series on Global Modeling and Data Assimilation, NASA Tech. Rep. TM-1999-104606.
- Cuvelier, C., Thunis, P., Vautard, R., Amann, M., Bessagnet, B., Bedogni, M., Berkowicz, R., Brocheton, F., Builtjes, P., Denby, B., Douros, G., Graf, A., Honoré, C., Jonson, J., Kerschbaumer, A., de Leeuw, F., Moussiopoulos, N., Philippe, C., Pirovano, G., Rouil, L., Schaap, M., Stern, R., Tarrason, L., Vignati, E., Volta, L., White, L., Wind, P., Zuber, A., 2006. CityDelta: a model intercomparison study to explore the impact of emission reductions in European cities in 2010. *Atmos. Environ.* 41, 189–207. <http://dx.doi.org/10.1016/j.atmosenv.2006.07.036>.
- (Ph.D. thesis) De Meij, A., 2009. Uncertainties in Modelling the Spatial and Temporal Variations in Aerosol Concentrations. Eindhoven University of Technology, the Netherlands (<http://alexandria.tue.nl/extra2/200911524.pdf>).
- De Meij, A., Wagner, S., Gobron, N., Thunis, P., Cuvelier, C., Dentener, F., 2007. Model evaluation and scale issues in chemical and optical aerosol properties over the greater Milan area (Italy), for June 2001. *Atmos. Res.* 85, 243–267.
- De Meij, A., Thunis, P., Bessagnet, B., Cuvelier, C., 2008. The sensitivity of the CHIMERE model to emissions reduction scenarios on air quality in Northern Italy. *Atmos. Environ.* 43, 1897–1907.
- De Meij, A., Gzella, A., Cuvelier, C., Thunis, P., Bessagnet, B., Vinuesa, J.F., Menut, L., Kelder, H.M., 2009. The impact of MM5 and WRF meteorology over complex terrain on CHIMERE model calculations. *Atmos. Chem. Phys.* 9, 6611–6632. <http://dx.doi.org/10.5194/acp-9-6611-2009>.
- Dosio, A., Galmarini, S., Graziani, G., 2002. Simulation of the circulation and related photochemical ozone dispersion in the Po plains (northern Italy): comparison with the observations of a measuring campaign. *J. Geophys. Res.* 107 (D18), 8189.
- Farr, T.G., et al., 2007. The Shuttle Radar Topography Mission. *Rev. Geophys.* 45, RG2004. <http://dx.doi.org/10.1029/2005RG000183>.
- Fraedrich, K., Kleidon, A., Lunkeit, F., 1999. A green planet versus a desert world: estimating the effect of vegetation extremes on the atmosphere. *J. Clim.* 12, 3156–3163.
- Goerber, M., Milton, S., 2002. On the use of radar data to verify Mesoscale Model precipitation forecasts. Report of the SRNWP workshop on mesoscale verification 2001, pp. 18–27. <http://dx.doi.org/10.1175/MWR3199.1>.
- Haywood, J.M., Ramaswamy, V., 1998. Global sensitivity studies of the direct radiative forcing due to anthropogenic sulfate and black carbon aerosols. *J. Geophys. Res.* 103, 6043–6058.
- Heymann, Y., Steenmans, Ch., Croissille, G., Bossard, M., 1994. CORINE land cover. Technical Guide EUR12585Office for Official Publications of the European Communities, Luxembourg.
- Hong, S.Y., Lim, J.O.J., 2006. The WRF single-moment 6-class microphysics scheme (WSM6). *J. Korean Meteor. Soc.* 42, 129–151.
- Hong, S.-Y., Noh, Y., Dudhia, J., 2006. A new vertical diffusion package with an explicit treatment of entrainment processes. *Mon. Weather Rev.* 134, 2318–2341.
- ISTAT (Italian National Institute of Statistics).). <http://www.istat.it/en/files/2011/06/Italy2012.pdf>.
- Jarvis, A., Reuter, H.I., Nelson, A., Guevara, E., 2008. Hole-Filled Seamless SRTM Data V4, International Centre for Tropical Agriculture (CIAT). (available from <http://srtm.csi.cgiar.org>).
- Kalnay, et al., 1996. The NCEP/NCAR 40-year reanalysis project. *Bull. Am. Meteorol. Soc.* 77, 437–470.
- Kim, Y., Sartelet, K., Raut, J.-C., Chazatte, P., 2013. Evaluation of the Weather Research and Forecast/Urban Model over Greater Paris. Bound.-Layer Meteorol. 149, 105–132. <http://dx.doi.org/10.1007/s10546-013-9838-6>.
- Lee, S.H., Kim, S.W., Angevine, W., Bianco, L., McKeen, S., Senff, C., Trainer, M., Tucker, S., Zamora, R., 2010. Evaluation of urban surface parameterizations in the WRF model using measurements during the Texas Air Quality Study 2006 field campaign. *Atmos. Chem. Phys.* 11, 2127–2143.
- Minguzzi, E., Bedogni, M., Carnevale, C., Pirovano, G., 2005. Sensitivity of CTM simulations to meteorological input. *Int. J. Environ. Pollut.* 24, 36–50.
- Mlawer, E.J., Taubman, S.J., Brown, P.D., Iacono, M.J., Clough, S.A., 1997. Radiative transfer for inhomogeneous atmospheres: RRTM, a validated correlated-k model for the longwave. *J. Geophys. Res.* 102 (D14), 16663–16682. <http://dx.doi.org/10.1029/97JD00237>.
- Penner, J.E., Chuang, C.C., Grant, K., 1998. Climate forcing by carbonaceous and sulfate aerosols. *Clim. Dyn.* 14, 839–851.
- Pineda, N., Jorba, O., Jorge, J., Baldasano, J.M., 2004. Using NOAA AVHRR and SPOT VGT data to estimate surface parameters: application to a mesoscale meteorological model. *Int. J. Remote Sens.* 25 (1), 129–143.
- Ritter, M., Mathias, D., Müller, M.D., Tsai, M.-Y., Parlow, E., 2013. Air pollution modeling over very complex terrain: an evaluation of WRF-Chem over Switzerland for two 1-year periods. *Atmos. Res.* 132–133, 209–222.
- Saha, S., et al., 2010. NCEP Climate Forecast System Reanalysis (CFSR) 6-hourly Products, January 1979 to December 2010. Research Data Archive at the National Center for Atmospheric Research, Computational and Information Systems Laboratory (<http://rda.ucar.edu/datasets/ds093.0>. Accessed 15-01-2014).
- Stephenson, David B., 2000. Use of the “odds ratio” for diagnosing forecast skill. *Weather Forecast.* 15, 221–232. [http://dx.doi.org/10.1175/1520-0434\(2000\)015<0221:UOTORF>2.0.CO;2](http://dx.doi.org/10.1175/1520-0434(2000)015<0221:UOTORF>2.0.CO;2).
- Stern, R., Builtjes, P., Schaap, M., Timmermans, R., Vautard, R., Hodzic, A., Memmesheimer, M., Feldmann, H., Renner, E., Wolke, R., Kerschbaumer, A., 2008. A model inter-comparison study focussing on episodes with elevated PM10 concentrations. *Atmos. Environ.* 42 (19), 4567–4588.
- Textor, C., Schulz, M., Guibert, S., Kinne, S., Bauer, S., Balkanski, Y., Berntsen, T., Berglen, T., Boucher, O., Chin, M., Dentener, F., Diehl, T., Feichter, H., Fillmore, D., Ghan, S., Ginoux, P., Gong, S., Grini, A., Hendricks, J., Horowitz, L., Isaksen, I., Iversen, T., Kirkevag, A., Koch, D., Kristjansson, J. E., Krol, M., Lauer, A., Lamarque, J.F., Liu, X., Montanaro, V., Myhre, G., Penner, J., Pitari, G., Reddy, S., Seland, O., Stier, P., Takemura, T., Tie, X., 2006. Analysis and quantification of the diversities of aerosol life cycles within AeroCom. *Atmos. Chem. Phys.* 6, 1777–1813. <http://dx.doi.org/10.5194/acp-6-1777-2006>.
- Thunis, P., Rouil, L., Cuvelier, C., Stern, R., Kerschbaumer, A., Bessagnet, B., Schaap, M., Builtjes, P., Tarrason, L., Douros, J., Moussiopoulos, N., Pirovano, G., Bedogni, M., January 2007. Analysis of model responses to emission-reduction scenarios within the CityDelta project. *Atmos. Environ.* 41 (1), 208–220.
- Tsyro, S.G., 2003. Model performance for particulate matter. EMEP Status report 1/2003. Transboundary Acidification, Eutrophication and Ground Ozone Level, Part II: Unified EMEP Model Performance. EMEP/MSC-W Status Report 1/2003 Part II. Norwegian Meteorological Institute, Oslo, Norway (http://emeep.int/publ/reports/2003/emeep_report_1_part2_2003.pdf).
- Van den Hurk, B.J.J.M., 1995. Sparse Canopy Parameterizations for Meteorological Models. (Ph.D. thesis) Wageningen Agricultural University, Wageningen.
- Van Loon, M., Roemer, M., Builtjes, P., 2004. Model intercomparison in the framework of the review of the Unified EMEP model. TNO-Report R 2004/282.
- Vautard, R., Thunis, P., Cuvelier, C., 2006. Evaluation and intercomparison of Ozone and PM10 simulations by several chemistry-transport models over 4 European cities within the CityDelta project. *Atmos. Environ.* 41, 173–188. <http://dx.doi.org/10.1016/j.atmosenv.2006.07.039>.
- Vautard, R., Builtjes, P., Thunis, P., Cuvelier, K., Bedogni, M., Bessagnet, B., Honore', Moussiopoulos, N., Schaap, M., Stern, R., Tarrason, L., van Loon, M., 2007. Evaluation and intercomparison of Ozone and PM10 simulations by several chemistry-transport models over 4 European cities within the City-Delta project. *Atmos. Environ.* 41, 173–188.
- Vautard, R., Schaap, M., Bergström, R., Bessagnet, B., Brandt, J., Builtjes, P.J.H., Christensen, J.H., Cuvelier, C., Foltescu, V., Graff, A., Kerschbaumer, A., Krol, M., Roberts, P., Rouil, L., Stern, R., Tarrason, L., Thunis, P., Vignati, E., Wind, P., October 2009. Skill and uncertainty of a regional air quality model ensemble. *Atmos. Environ.* 43 (31), 4822–4832.
- West, J.J., Pilinis, C., Nenes, A., Pandis, S.N., 1998. Marginal direct climate forcing by atmospheric aerosols. *Atmos. Environ.* 32, 2531–2542.